Convergent Synthesis of a Hexadecavalent Heterobifunctional ABO Blood Group Glycoconjugate

Gour Chand Daskhan, Hanh-Thuc Ton Tran, Christopher W. Cairo*

Department of Chemistry, University of Alberta, Edmonton Alberta, T6G 2G2, Canada

*To whom correspondence should be addressed. Tel.: 780 492 0377; fax: 780 492 8231; e-mail: ccairo@ualberta.ca

ABSTRACT

Naturally occurring glycans are often found in a multivalent presentation. Cell surface receptors that recognize these displays may form clusters, which can lead to signalling or endocytosis. One of the challenges in generating synthetic displays of multivalent carbohydrates is providing high valency as well as access to heterofunctional conjugates to allow attachment of multiple antigens or payloads. We designed a strategy based on a set of bifunctional linkers to generate a heterobifunctional multivalent display of two carbohydrate antigens to bind BCR and CD22 with four and twelve antigen copies, respectively. We confirmed that the conjugates were able to engage both CD22 and BCR on cells by observing receptor clustering. The strategy is modular and would allow for alternative carbohydrate antigens to be attached bearing amine and alkyne groups and should be of interest for the development of immunomodulators and vaccines.

Graphical abstract

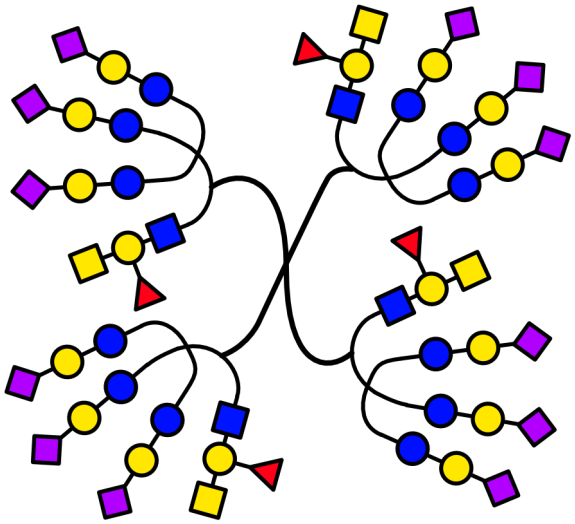

Highlights

- Synthesis of a hexadecavalent display of carbohydrate antigens
- Modular strategy to display two separate epitopes in a multivalent conjugate
- Increased valency of CD22 ligands induces receptor clustering on cells

1. INTRODUCTION

Naturally occurring glycans are often found in multivalent and heterogenous presentations on proteins and lipids.[1,2] The nature of this presentation allows for increased avidity in lectin binding and may aid in discrimination between specific glycan epitopes.[3–7] Bioconjugate chemists have developed synthetic strategies to mimic multivalent glycan displays that have included dimers, tetramers, linear polymers, branched polymers, surfaces, liposomes, and nanoparticles.[5,8–14] The development of discrete multivalent presentations of glycans has expanded in recent years allowing access to supramolecular glycan displays that mimic natural glycoconjugates.[11,15–17] One of the challenges in development of these targets is access to heterofunctional conjugates that allow for the display of multiple epitopes with discrete stoichiometries.

Heterofunctional multivalent displays can be used to engage multiple biological targets simultaneously, and can be critical to the design of vaccines and reagents to modulate receptor signaling.[10,17–19] Heterofunctional conjugates may carry a single antigen along with a payload or label; alternatively they may be used to engage multiple receptors simultaneously to induce receptor clusters. An example of the latter strategy has involved the display of a B cell receptor (BCR) antigen on a conjugate that can engage the CD22 co-receptor.[20–23] CD22 is a Siglec which can attenuate BCR signaling, making conjugates of this form potential immunomodulators.[24–26] Linear polymers generated by stoichiometric control with two epitopes have been used to investigate BCR and CD22 co-clustering.[22,23,27,28] Larger IgM, liposome, and nanoparticle complexes have been used to target BCR and CD22,[20,21,29–33] and CD22 ligands displayed on N-glycan structures have been used for targeted delivery of toxins to cells.[34] A heterobifunctional display of

three copies of a nitrophenyl antigen and three copies of a high-affinity CD22 ligand has been reported,[35] and more recently dimeric CD22 ligands have been developed.[36]

Our group has been interested in the development of heterobifunctional glycoconjugates that allow presentation of multiple carbohydrate antigens for controlling receptor organization. Specifically, we developed a heterobifunctional linker that allowed elaboration of a tetravalent PEG scaffold with two carbohydrate ligands: a 6'-sialyl-lactose (6'SL) ligand for CD22, and a human A type II (AII) blood group antigen.[37] Using a human B cell clone that expresses an AII-specific BCR, known as A-BCL,[38] we were able to demonstrate co-clustering of BCR with CD22 using these ligands.[37] We later modified our strategy to improve the persistence of these glycoconjugates in vivo through the addition of a serum-protein binding ligand and fluorophore.[39] Targeting of CD22 receptors with multivalent displays is often observed to require high affinity or high avidity ligands to overcome interactions of the receptor with *cis* sialosides.[40] As a result, we considered ways to modify our strategy to provide increased valency of the CD22 ligand. We envisioned that modification of our bifunctional linker to allow attachment of multiple copies of the CD22 ligand would provide access to a dodecavalent display of sialosides while providing a tetravalent display of the BCR-specific antigen (**Figure 1**). Unlike our original tetravalent design, we found that the hexadecavalent conjugates were able to independently cluster CD22 on B cells without the requirement of a BCR-specific antigen. This expansion of our synthetic strategy should allow for the design of improved multivalent conjugates to engage CD22 and BCR.

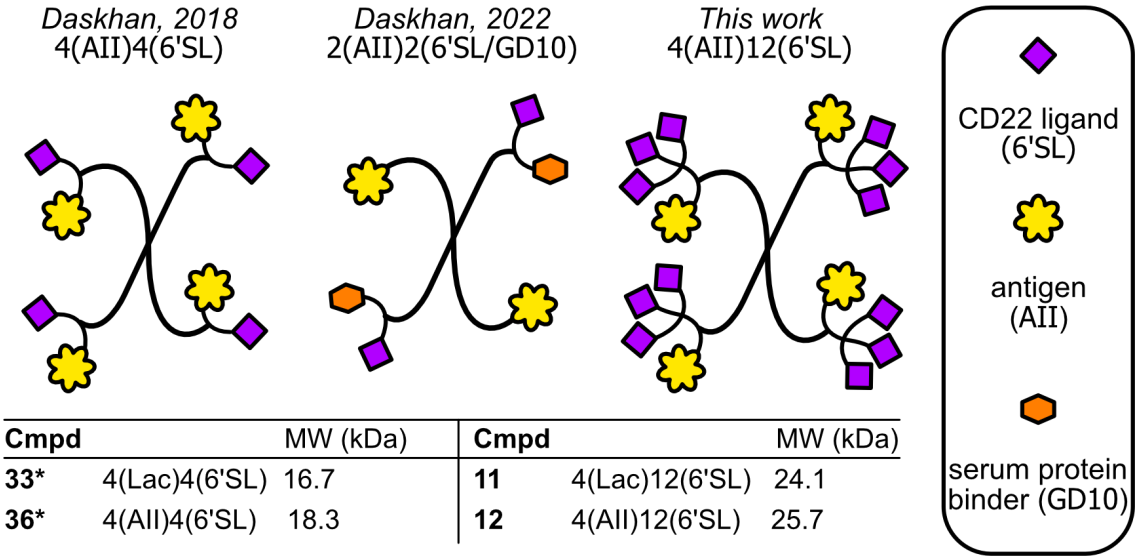

Cmpd		MW (kDa)	Cmpd		MW (kDa)
33*	4(Lac)4(6'SL)	16.7	**11**	4(Lac)12(6'SL)	24.1
36*	4(AII)4(6'SL)	18.3	**12**	4(AII)12(6'SL)	25.7

Figure 1: Schematic overview of glycoconjugates based on a tetravalent core. Glycoconjugates were designed to simultaneously engage CD22 receptors and BCR (IgM) on B cells. Conjugates with four copies of a bivalent display of the carbohydrate antigen (Lac or AII) and a CD22 ligand (6'SL) were reported previously.[37] Modified conjugates that contained a copy of a serum protein binder were used to extend the half-life of conjugates in vivo.[39] In this work, we generate higher valency displays of the CD22 ligand with four copies of the carbohydrate antigen. A summary of the final conjugates discussed here is given with the number of antigen and ligand copies and average molecular weight. *Compounds first reported by Daskhan et al., and conjugate numbering is maintained from that work for clarity.[37]

2. RESULTS AND DISCUSSION

2.1 Design and synthesis of a tetrafunctional linker

We set out to synthesize a hexadecavalent heterobifunctional glycoconjugate using a convergent approach. We required a suitable tetrafunctional linker featuring a handle for attachment of three copies of a ligand and an orthogonal group for attachment to the scaffold. We designed linker **4** terminated with three azido groups and an amine based on previous work with *N*α-Fmoc-*N*ε-azido-L-lysine (Fmoc-Lys(N_3)-OH, **1**).[37] Fmoc-Lys(N_3)-OH (**1**) was coupled directly to acid-labile 2-chlorotrityl chloride resin in the presence of DIPEA in CH_2Cl_2 followed by Fmoc deprotection with piperidine. Subsequent coupling of Fmoc-Lys(N_3)-OH **1** with HBTU provided the resin-bound form of compound **2**.[41] Cleavage from the resin with 95% trifluoroacetic acid (TFA) afforded acid **2** in quantitative yield after purification by silica gel chromatography. Acid **2** was converted to its *N*-hydroxysuccinimidyl (NHS) ester through reaction with NHS and dicyclohexylcarbodiimide (DCC) in CH_2Cl_2 to afford **3** in 82% yield after purification. The coupling of commercially available 3-azido-1-propanamine with **3** in the presence of DIPEA in anhydrous DMF was followed by removal the Fmoc-protecting group with 20% piperidine in DMF at room temperature to afford **4** in a 75% overall yield after semi-preparative RP-HPLC purification (**Scheme 1**).

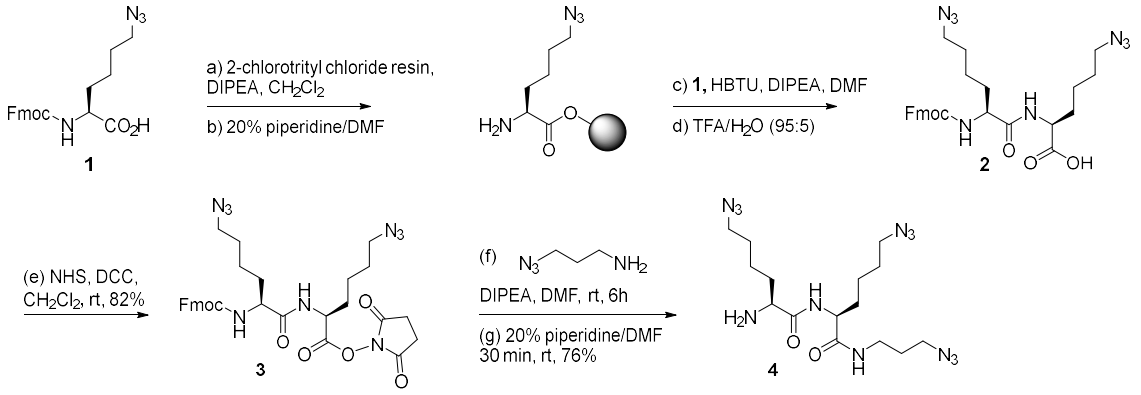

Scheme 1. Synthesis of tetrafunctional linker **4**

2.2 Synthesis of a trivalent display of 6'sialyllactose

To prepare a trivalent sialoside bearing an alkyne moiety (**8**), we implemented a CuAAC ligation strategy developed previously in our group.[37,39] The CuAAC ligation of tetravalent linker **4** bearing three copies of the azide moiety with 6'-sialyllactose (6'SL, **5**) (1.25 equiv per N_3) was carried out in the presence of Cu-powder (10 equiv per N_3) in PBS buffer (pH 7.4) at room temperature under an inert atmosphere. After Sep-pak C-18 purification, amine-containing trivalent sialoside **6** (2,424 Da) was isolated in 87% yield. Formation of the desired product was confirmed by ^{1}H NMR and HRMS. The alkyne functionality was introduced at the free amine of sialoside **6** through coupling with 2 equivalents of propargyl-*N*-hydroxysuccinimidyl ester **7** in the presence of DIPEA in anhydrous DMF at 37 ºC overnight. Upon completion, the crude product was purified using P-2 gel chromatography to afford trivalent conjugate **8** in 81% yield as an off-white powder after lyophilisation (**Scheme 2**). Formation of the trivalent structure was confirmed through analysis of ESI-HRMS and ^{1}H NMR.

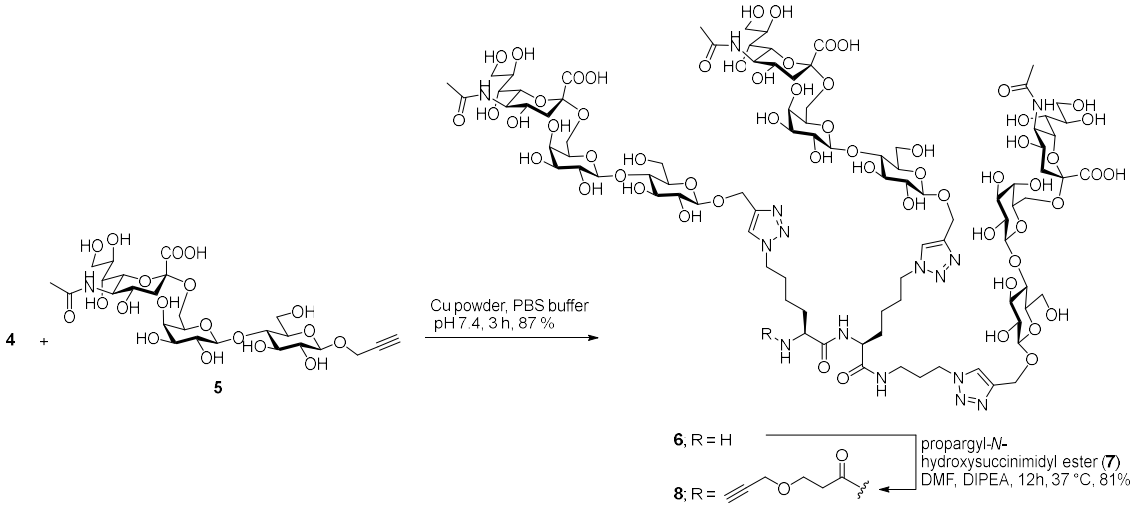

Scheme 2. Synthesis of alkyne-bearing trivalent sialoside **8**

2.3 Synthesis of Hexadecavalent glycoconjugates

A new series of synthetic hexadecavalent scaffolds (**11** and **12**) were selected to evaluate the influence of valency and architecture for testing in BCR-CD22 co-clustering by cell-imaging. Two different high valent glycoconjugates displaying 4 copies of A-type II antigen (or a lactose control) and 12 copies of the 6'-sialyllactose (6'SL) were synthesized by employing a highly efficient convergent strategy. The strategy required the CuAAC coupling of the alkyne-functionalized trivalent sialoside **8** with the tetravalent structures displaying 4 copies of the azide moiety on a PEG scaffold. For this purpose, A-type II and lactose groups with an amino linker were first conjugated to a trifunctional linker as previously described.[37] Subsequent reaction of our linker with the commercially available tetravalent NHS-activated PEG scaffold provided the tetravalent lactose conjugate **9** (14.1 kDa) and A-type II conjugate **10** (15.7 kDa) displaying 4 copies of the azide moiety (**Scheme 3**).[37] Ligation of this tetravalent azide by CuAAC to the trivalent sialoside display in compound **8** provided hexadecavalent heterobifunctional structures **11** and **12**. The reaction was catalyzed with Cu-powder (10 equiv per azide) in the presence of the trivalent sialoside **8** (1.25 equiv

per N_3) and tetravalent structures **9** or **10** in PBS buffer (pH 7.4) under vigorous stirring and bubbled with N_2 gas. After purification with P-2 gel, conjugates **11** (24.1 kDa) and **12** (25.7 kDa) were isolated in 88% and 90% yields, respectively. The stoichiometry of the heterobifunctional hexadecavalent glycoconjugates **11** and **12** were confirmed by ^{1}H NMR integration of the triazole H5 (8.0 ppm, broad singlet), lactosyl H1 (4.5, 4.3 or 5.3, 5.1 ppm), PEG methylene (2.4 ppm), and NHAc peaks (1.99 ppm).

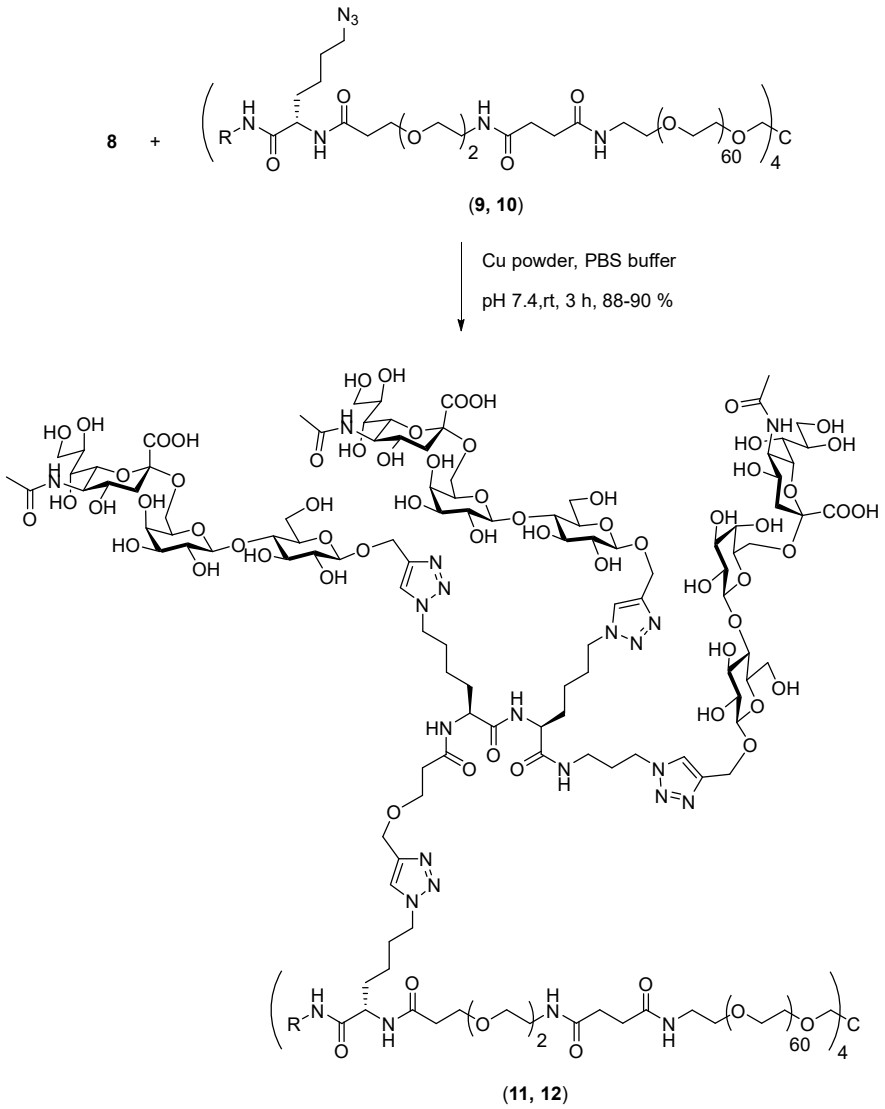

Entry (carbohydrate antigen)	Reactant	R-NH_2	CuAAC product	yield and average mol. weight (kDa)
1 (lactose)	**9**	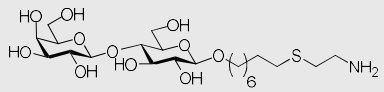	**11**	(88%, 24.1)
2 (AII)	**10**	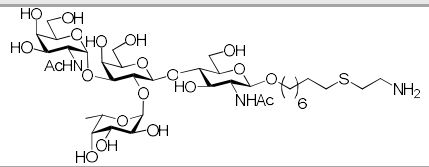	**12**	(90%, 25.7)

Scheme 3. Synthesis of hexadecavalent conjugates **11** and **12** using a convergent strategy.

2.4 Clustering of IgM and CD22 receptors by glycoconjugates

With conjugates **11** and **12** in hand, we proceeded to evaluate the ability of these compounds to induce clustering of IgM and CD22 receptors. In our previous work we used the A-BCL model, which expresses an AII-specific BCR.[38] Using PEG conjugates we found that the presence of both a BCR-specific antigen and a CD22 ligand (6'SL) was required for clustering of CD22 receptors by low-valency conjugates (2 and 4 copies of 6'SL).[37,39] This is likely due to a requirement for high avidity ligands to overcome *cis* interactions of CD22 on the B cell membrane.[40] For examples, high valency CD22 ligands alone clustered CD22 receptors when using a polyacrylamide display of sialic acid.[37,42] Thus, we expected that increasing the copy numbers of CD22 ligands on our PEG scaffold could cluster CD22 even in the absence of BCR-specific antigens. To test this hypothesis, we tested the ability of glycoconjugate **11** (4(Lac)12(6'SL)) with each arm of the scaffold carrying 3 copies of 6'SL and one copy of lactose as a negative control antigen to cluster CD22. As shown in **Figure 2**, CD22 receptors were dispersed on the cell membrane in microclusters in untreated A-BCL cells. Although conjugate **33** (4(Lac)4(6'SL)) was unable to cluster CD22, the higher copy number of the CD22 ligand in conjugate **11** (4(Lac)12(6'SL)) generated significantly increased CD22 clusters. This result confirms that 12 copies of CD22 ligand were sufficient to induce clustering in the absence of specific BCR antigen.[42] Consistent with previous observations, the addition of a BCR-specific antigen to the tetravalent display of CD22 ligand in conjugate **36** (4(AII)4(6'SL)) resulted in clustering of CD22 and BCR on cells.[37] Testing of glycoconjugate **12** (4(AII)12(6'SL)) maintained or increased clustering of CD22 and BCR on A-BCL cells (**Figures 2 & 3; Table 1**). Although conjugate **12** increased CD22 cluster size relative to control treatment, these clusters were not significantly different from those induced by conjugate **36**.

Our experiments confirmed that glycoconjugates bearing CD22 ligands of sufficient valency can induce CD22 clustering, and that a BCR-specific antigen is required to induce BCR clusters.[37,40] In the present work we find that the threshold for forming CD22 clusters on A-BCL cells was met with 12 copies of 6'SL ligand per scaffold. The development of a synthetic strategy to generate defined supramolecular displays of CD22 ligands combined with a BCR antigen should allow future experiments to better understand the role of receptor co-clustering and organization in immune signaling.[11,22,23]

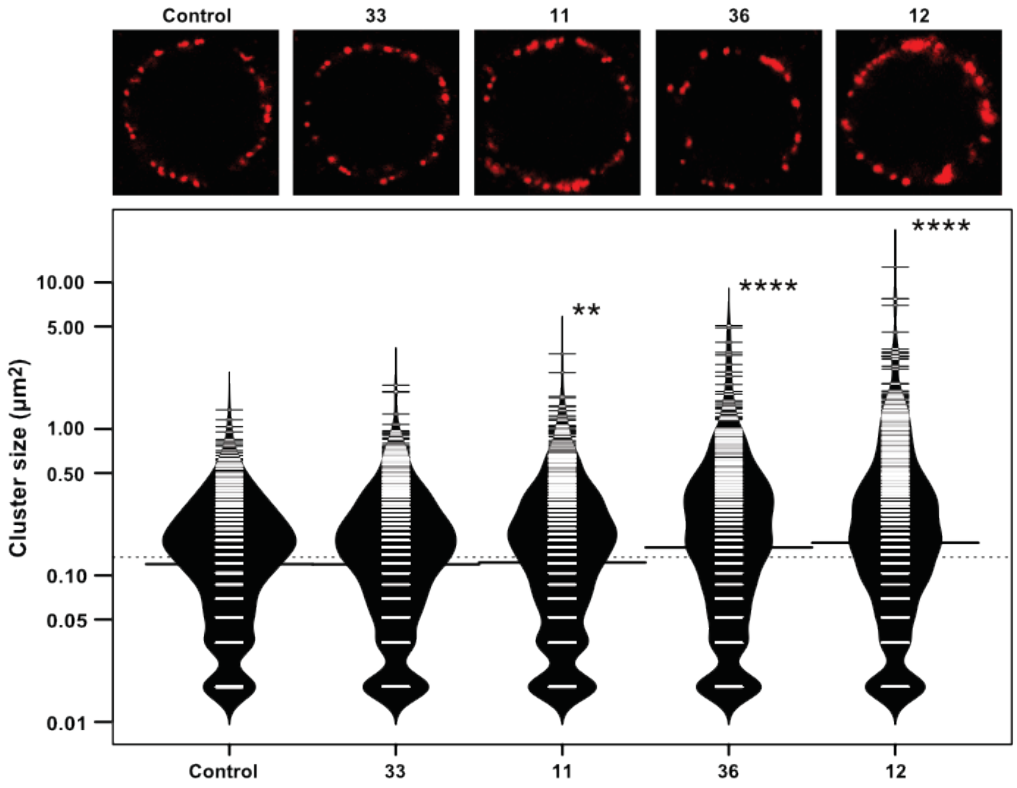

Figure 2. Clustering of CD22 receptors by glycoconjugates. A-BCL cells were treated with PBS containing 25 ng mL^{-1} **33, 11, 36,** or **12**, then fixed and stained with anti-CD22 (mouse) and visualized using confocal microscopy. (**A**) Confocal fluorescence images of representative cells are shown for each treatment. (**B**) Cluster sizes on 20 individual cells were determined using particle analysis in ImageJ and plotted using the beanplot statistical package in R.[37,39,43] Each individual white horizontal line within the beanplot represents one single data point, the black horizontal line indicates the mean for each condition, and the dotted line indicates the mean of all conditions within the plot. Populations which were statistically different from control based on a Student's t-test are indicated (**, $p < 0.05$; ****, $p < 0.0001$.) Data shown were pooled from three biological replicates.

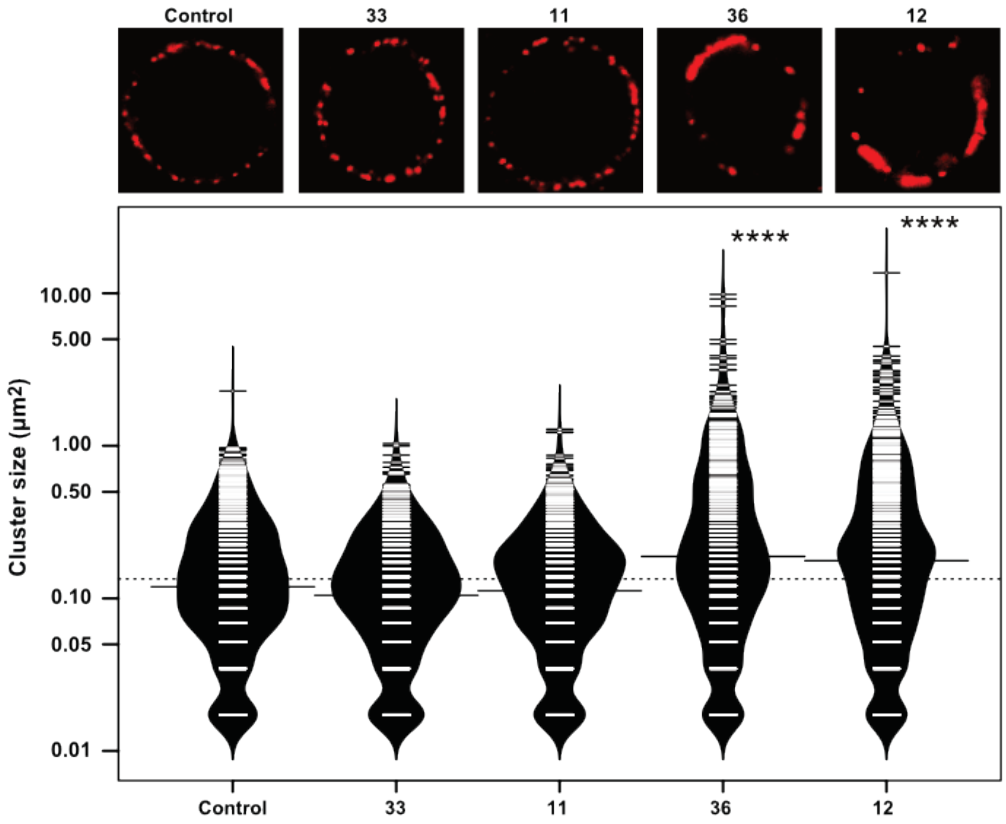

Figure 3. Clustering of IgM receptors by glycoconjugates. A-BCL cells were treated with PBS containing 25 ng mL^{-1} **33, 11, 36, or 12**, then fixed and stained with anti-IgM (mouse) and visualized using confocal microscopy. (**A**) Confocal fluorescence images of representative cells are shown for each treatment. (**B**) Cluster sizes on 20 individual cells were determined using particle analysis in ImageJ and plotted using the beanplot statistical package in R.[37,39,43] Each individual white horizontal line within the beanplot represents one single data point, the black horizontal line indicates the mean for each condition, and the dotted line indicates the mean of all conditions within the plot. Populations which were statistically different from control based on a Student's t-test are indicated (****, $p < 0.0001$.) Data shown were pooled from three biological replicates.

Table 1: Clustering of BCR and CD22 receptors by high-valent conjugates

Compound	***Name/Antigen[a]***	***IgM[b]***	***n***	***cluster[c]***	***CD22[b]***	***n***	***cluster[c]***
-	control	0.18 ± 0.02	687	-	0.18 ± 0.02	661	-
11	4(Lac)12(6'SL)	0.17 ± 0.02	739	-	0.21 ± 0.03	831	+
12	4(AII)12(6'SL)	0.40 ± 0.1	633	+	0.38 ± 0.1	719	+
33[d]	4(Lac)4(6'SL)	0.15 ± 0.02	582	-	0.19 ± 0.02	851	-
36[d]	4(AII)4(6'SL)	0.45 ± 0.1	540	+	0.32 ± 0.1	498	+

a. Antigens on synthetic conjugates are listed in parenthesis, with the copy number preceding. Abbreviations used are: lactose, Lac; A-type II, AII; 6'-sialyllactose, 6'SL.

b. Mean cluster size [μm^2] of the indicated receptor was determined as described in materials and methods.

c. The value of n refers to the number of individual clusters detected in the images from 20 cells for each condition. If the mean cluster size was statistically larger ($p < 0.05$ by the Student's t-test) for the indicated receptor after treatment with a protein or conjugate, it is indicated with a "+".

d. Compounds prepared in previous work,[37] were tested in these experiments for comparison.

3. CONCLUSIONS

We report a convergent synthetic strategy to access hexadecavalent displays of a CD22 ligand (6'SL) with a separate tetravalent display of a BCR-specific antigen (AII). The heterobifunctional conjugates were able to engage both CD22 and BCR on a B cell model. Importantly, the increased valency of the CD22 ligand display allowed for clustering of CD22 even in the absence of a BCR-specific antigen. The synthetic strategy used here is modular and can be easily adapted for other bifunctional displays where the antigens have either an amine or alkyne functionality to link to the scaffold.

4. EXPERIMENTAL PROCEDURES

4.1 General Methods

Reagents were purchased from commercial sources as noted and used without additional purification. NHS-activated tetravalent PEG scaffolds were purchased from Laysan Bio Inc, Arab, Alabama 35016. Fmoc-Lys-OH, Cu-powder (< 425 μm), propargyl-*N*-hydroxysucinimidyl ester **7**, and DIPEA were purchased from Sigma-Aldrich, Canada. Fmoc-9-amino-4,7-dioxanonanoic acid was purchased from ChemPep Inc. HBTU and 2-chlorotrityl chloride resins were purchased from Novabiochem. Deuterated chloroform-d_1 and D_2O were purchased from Deutero GmbH. Other solvents (analytical and HPLC grade) and reagents were purchased from Aldrich and were used as received. Conjugates **9**, **10**, **33**, and **36** were prepared as previously described; these compounds were numbered as **23**, **26**, **33**, and **36**, respectively, in the original report.[37] Reactions were conducted under a stream of argon at ambient temperature unless otherwise noted, and reactions were monitored by analytical TLC on silica gel 60-F254 (0.25 nm, Silicycle, QC, Canada). Developed TLC plates were visualized under UV lamp (λ_{max} = 254 nm) and charred by heating plates that were dipped in

ninhydrin solution in ethanol, and acidified anisaldehyde solution in ethanol. Reaction products were purified by silica gel column chromatography (230-400 mesh, Silicycle, QC, Canada) or size exclusion chromatography using Bio-Gel P-2 Gel from Bio-Rad Laboratories (Canada) Ltd. Ontario, Canada, or C-18 Sep-pak chromatography using ethyl acetate/hexane, or CH_2Cl_2/MeOH and MeOH/H_2O as mobile phase, respectively. Semi-preparative RP-HPLC was performed with a Waters Delta 600 pump and a Waters 600 controller with Empower 2 software. Eluted peaks were detected with a Waters 2420 evaporative light scattering (ELS) detector or a Waters 2996 photodiode array (PDA) detector (Waters Ltd., Mississauga, ON, Canada). Mobile phase was solvent A: 0.01% TFA in water, and solvent B: CH_3CN at a flow rate of 8.0 mL min^{-1} using a linar gradient of 2-50% solvent B over 20 min and UV detection at 214 nm. NMR experiments were conducted on a Varian 500 or 600 MHz instruments in the University of Alberta Chemistry NMR Facility. Chemical shifts are reported relative to the deuterated solvent peak or 3-(trimethylsilyl)-propionic-2,2,3,3-d_4 acid sodium salt as an internal standard and are in parts per million (ppm). Coupling constants (J) are reported in Hz and apparent multiplicities were described in standard abbreviations as singlet (s), doublet (d), doublet of doublets (dd), triplet (t), broad singlet (bs), or multiplet (m). Electrospray mass spectra (ESI-MS) were recorded on Agilent Technologies 6220 TOF.

4.2 General procedure for CuAAC ligation

A solution of azide-terminated PEG-conjugate (1 equiv) and propargyl sialoside (1.25 equiv per N_3) in PBS buffer (5-10 mM, pH 7.4) was bubbled with N_2 for 30 min at room temperature. Cu-power (12 equiv per N_3) was added to the solution under an argon atmosphere and the reaction mixture was left stirring vigorously for an additional 3 h at room temperature. The progress of the coupling was monitored by TLC and UPLC for disappearance of the propargyl sialoside. After completion, the solution was filtered through

a two-micron filter and the crude product was purified by Bio-Gel P-2 gel chromatography using H_2O eluent to afford the conjugate as an off-white powder after lyophilization.

4.3 *Solid-phase synthesis of linker* ***2****, (2S)-6-azido-2-[(2S)-6-azido-2-({[(9H-fluoren-9-yl)methoxy]carbonyl}amino)hexanamido]hexanoic acid*

Fmoc-Lys(N_3)-OH (**1**) was prepared using imidazole-1-sulphonyl azide as the diazotransfer reagent following a previously reported procedure.[44,45] The dipeptide was prepared using solid phase peptide synthesis protocol starting from Fmoc-Lys(N_3)-OH (**1**) and 2-chlorotrityl chloride resin. Coupling reactions were performed using 2-chlorotrityl chloride resin (500 mg, 0.65 mmol) and Fmoc-Lys(N_3)-OH **1** (2 equiv) in the presence of HBTU (2 equiv) and DIPEA (3 equiv) in CH_2Cl_2 and DMF (10 mL g^{-1} resin), respectively, for 45 min. After each reaction the resin beads were repeatedly washed with DMF (10 mL, 4 times) to remove excess amino acid and coupling reagent. Progress of the coupling reaction was monitored by the TNBS test using a solution of trinitrobenzenesulfonic acid in DMF (1%). The *N*-Fmoc protecting group was removed by treatment with 20% piperidine-DMF (10 mL 1:4, v/v, g^{-1} resin) for 15 min. The linear dipeptide was cleaved from resin treated with a cleavage cocktail TFA: H_2O (4 x 2 mL, 9:5:0.5) for 2 h. The combined cleavage solutions were concentrated under vacuum and the crude product was purified by silica gel chromatography using ethyl acetate as eluent to afford peptide **2** (402 mg, 79%) as a colorless oil. R_f = 0.42 (EtOAc/MeOH = 9.5:0.5); ^{1}H NMR (600 MHz, $CDCl_3$): δ 7.78 (d, J = 7.8 Hz, 2H), 7.59 (d, J = 7.2 Hz, aromatic H, 2H), 7.42 (t, J = 7.2 Hz, aromatic H, 2H), 7.34-3.31 (m, aromatic H, 2H), 6.83 (d, J = 6.6 Hz, CH_2-, 1H), 5.63 (d, J = 9.6 Hz, 1H), 4.59 (dd, J = 15.6, 8.4 Hz, 1H), 4.46-4.37 (m, 2H), 4.27 6.83 (d, J = 7.8 Hz, 1H), 4.23-4.21 (m, 1H), 3.27 (t, J = 7.8 Hz, 2H), 3.22 (t, J = 7.8 Hz, 2H), 1.96-1.92 (m, 1H), 1.88-1.82 (m, 1H), 1.76-1.68 (m, 1H), 1.61-1.56 (m, 5H), 1.43-1.42 (m, 2H); ^{13}C NMR (125 MHz, $CDCl_3$): δ 174.03 (2CO),

171.80, 156.43, 143.65, 143.59, 141.32, 141.31, 127.83, 127.10, 125.03, 124.97, 120.07, 120.05, 67.37, 54.64, 52.07, 51.09, 50.97, 47.06, 32.02, 31.45, 28.39, 28.29, 22.55, 22.41; HRMS (ESI): m/z $[M+Na]^+$ calcd for C27H31N8O5-H: 547.2425, found: 547.2415.

*4.4 Synthesis of compound **3**, 2,5-dioxopyrrolidin-1-yl (2S)-6-azido-2-[(2S)-6-azido-2-({[(9H-fluoren-9-yl)methoxy]carbonyl}amino)hexanamido]hexanoate*

N-Hydroxysuccinimide (52.5 mg, 0.45 mmol) was added to a solution of compound **2** (200 mg, 0.36 mmol) and *N,N*-dicyclohexylcarbodiimide (94 mg, 0.45 mmol) in CH_2Cl_2 (8 mL) under an argon atmosphere at room temperature. After completion, the crude solution was filtered through a celite pad, the organic layer was washed with aq. HCl (2N) solution, then dried over sodium sulfate and evaporated to dryness. The crude product was purified by silica gel column chromatography using an ethyl acetate-hexane mobile phase (2:3) to provide linker **3** (405 mg, 86 %) as a colorless oil. R_f = 0.31 (cyclohexane/EtOAc = 3:2); ^{1}H NMR (600 MHz, $CDCl_3$): δ 7.78 (d, *J* = 7.2 Hz, aromatic H, 2H), 7.59 (d, *J* = 7.2 Hz, aromatic H, 2H), 7.42 (t, *J* = 7.2 Hz, aromatic H, 2H), 7.33 (t, *J* = 7.2 Hz, aromatic H, 2H), 7.04 (d, *J* = 7.2 Hz, N*H*-, 1H), 6.59 (s, C*H*-, 1H), 5.43 (d, *J* = 7.2 Hz, C*H*-, 1H), 4.98-4.94 (m, CH_2-, 1H), 4.46-4.38 (m, C*H*-, 2H), 4.22 (t, *J* = 6.6 Hz, CH_2-, 2H), 3.29-3.24 (m, 4H), 3.63 (bs, PEG CH_2-, 4H), 3.57-3.56 (m, PEG CH_2-, 2H), 3.99-3.37 (m, CH_2-, 2H), 3.28 (t, *J* = 6.6 Hz, CH_2-, 2H), 2,84 (s, NHS-CH_2-, 4H), 2.04-2.00 (m, CH_2-, 1H), 1.90-1.89 (m, CH_2-, 1H), 1.70-1.69 (m, CH_2-, 2H,), 1.64-1.59 (m, CH_2-, 2H), 1.55-1.51 (m, CH_2-, 2H), 1.46-1.44 (m, CH_2-, 2H); ^{13}C NMR (125 MHz, $CDCl_3$): δ 171.34, 168.46 (2CO), 167.55 (2CO), 143.70, 141.31, 156.53, 127.80 (2C), 127.10, 125.05, 124.98, 120.05, 120.03, 67.23, 54.59, 51.12, 50.95, 50.35, 47.11, 33.92, 31.93,31.73, 28.44, 28.20, 25.61, 25.57, 22.50, 22.20; HRMS (ESI): m/z $[M+Na]^+$ calcd for C31H35N9O7Na: 668.2552, found: 668.2561.

*4.5 Synthesis of tetrafunctional linker **4**,*

(2S)-2-[(2S)-2-amino-6-azidohexanamido]-6-azido-N-(3-azidopropyl)hexanamide

NHS-activated compound **3** (75.0 mg, 11.6 μmol) and 3-azido-1-propanamine (14.5 μL, 14.5 μmol) were dissolved in anhydrous DMF (200 μL) in a 5 mL RBF and to this solution DIPEA (~18.7 μL, 17.4 μmol) was added to adjust pH of the solution to 8.5. The reaction mixture was left stirring for 6 h at room temperature under anhydrous conditions. The solvent was evaporated to dryness and treated with a 20% solution of piperidine in DMF (1 mL, 2:8, v/v) for 1 h at room temperature. After completion, solvent was removed under vacuum and the crude product was purified by semi-preparative RP-HPLC to afford compound **4** (36.3 mg, 76%) as an off-white solid after lyophilization. Analytical RP-HPLC t_R = 8.2 min (gradient 5 to 100% B in 30 min); ^{1}H NMR (600 MHz, D_2O): δ 4.24 (t, *J* = 7.2 Hz, -COC*H*-, 1H), 3.98 (t, *J* = 6.6 Hz, -COC*H*-, 1H), 3.34-3.28 (m, -CH_2-N3, CH_2-, 6H), 1.88-1.84 (m, -CH_2, 2H), 1.77-1.70 (m, -CH_2, 4H), 1.62-1.55 (m, -CH_2, 4H), 1.43-1.33 (m, -CH_2, 4H); ^{13}C NMR (125 MHz, D_2O): δ 174.17 (CO), 170.50 (CO), 53.17, 53.82, 51.81, 51.63, 49.58, 37.61, 31.46, 31.41, 28.63, 28.58, 28.53, 23.32, 22.21; HRMS (ESI): m/z [M+H]+ calcd for C15H29N12O2: 409.2531, found: 409.2529; m/z $[M+Na]^+$ calcd for C15H29N12O2Na: 431.2350, found: 431.2354.

*4.6 Synthesis of trivalent sialoconjugate **6***

Conjugate **6** was obtained by coupling of linker **4** (10 mg, 24.49 μmol) with propargyl sialoside **5** (61.6 mg, 91.85 μmol)[37] by following a general procedure described for CuAAC ligation, in a 84% yield (51.8 mg) as an off-white foam after P-2 gel chromatography purification using eluent system H_2O and lyophilization. Coupling efficiency of the sialoside **6** was determined by ^{1}H NMR integration of the underlined peaks to be sialoside:linker = 3:1. ^{1}H NMR (600 MHz, D_2O): δ 8.01 (s, 1H), 4.93 (t, *J* = 12.6 Hz, 1H),

4.83-4.80 (m, 1H), 4.53-4.52 (m, 1H), 4.40-4.35 (m, 3H), 4.12 (t, *J* = 7.6 Hz, 1H), 3.91 (d, *J* = 8.4 Hz, 1H), 3.90 (d, *J* = 8.4 Hz, 1H), 3.84-3.75 (m, 7H), 3.66 (d, *J* = 10.2 Hz, 1H), 3.62-3.55 (band, 8H), 3.52-3.47 (m, 4H), 3.02 (board s, 11H), 3.41 (t, *J* = 7.6 Hz, 1H), 2.66 (dd, *J* = 12.0, 4.2 Hz, 1H), 2.06-2.03 (m, 1H), 1.97 (s, 3H, NHAc), 1.90-1.86 (m, 2H), 1.77 (t, *J* = 12.0 Hz, 2H), 1.73-1.71 (m, 2H), 1.69-1.65 (m, 1H), 1.28-1.24 (m, 2H); ^{13}C NMR (126 MHz, D_2O): δ 175.86 (CO), 174.70 (NH*C*OCH$_3$), 174.43 (CO), 140.50 (2C), 144.42, 126.33, 126.24, 126.22, 104.20, 102.21, 80.50, 75.65, 75.58, 74.64, 73.61, 73.50, 73.33, 72.76, 71.76, 69.48, 69.34, 69.32, 64.49, 63.61, 63.00, 61.21, 55.01, 55.77, 51.07, 49.84 (2C), 48.90, 41.08, 37.60, 31.45, 31.01, 28.43, 28.23, 28.12, 23.04, 22.01; HRMS (ESI): m/z [M+2H]+2 calcd for C93H153N152O59: 1211.9711, found: 1211.9718.

4.7 Synthesis of trivalent sialoside ***8***

Propargyl-*N*-hydroxysucinimidyl ester **7** (9.3 mg, 41.3 μmol) and compound **6** (50.0 mg, 20.6 μmol) were dissolved in anhydrous DMF (500 μL) in a 5 mL RBF and to this solution DIPEA (~4.0 μL, 30.9 μmol) was added to adjust pH of the solution to 8. The reaction mixture was incubated overnight at 37 °C under anhydrous conditions. The solvent was removed to dryness followed by a P-2 gel chromatography purification using H_2O as eluent and subsequent lyophilisation furnished the desired compound **8** in 81% yield (42.5 mg) as an off-white powder. Coupling efficiency of sialoside **8** was determined by ^{1}H NMR integration of the underlined peaks to be sialoside:linker = 3:1. ^{1}H NMR (600 MHz, D_2O): δ 8.04 (s, 1H), 4.93 (t, *J* = 12.6 Hz, 1H), 4.84-4.80 (m, 1H), 4.54-4.53 (m, 1H), 4.41-4.37 (m, 3H), 4.18 (t, *J* = 6.0 Hz, 1H), 4.14-4.10 (m, 1H), 3.93 (d, *J* = 8.4 Hz, 1H), 3.90 (d, *J* = 8.0 Hz, 1H), 3.88-3.84 (m, 1H), 3.79-3.70 (m, 6H), 3.69-3.63 (m, 1H), 3.62-3.56 (m, 12H), 3.51-3.48 (m, 4H), 3.02 (board s, 11H), 3.33-3.30 (m, 1H), 3.17-3.11 (m, 1H), 2.83 (t, *J* = 7.8 Hz, 1H, -C*H*), 2.65 (dd, *J* = 12.0, 4.2 Hz, 1H), 2.53-2.50 (m, 1H), 2.07-2.05 (m, 1H), 1.98 (s, 3H, NHAc), 1.90-1.83 (m, 2H), 1.77 (t, *J* = 12.0 Hz, 1H), 1.75-1.71 (m, 3H), 1.28-1.23 (m, 2H);

^{13}C NMR (126 MHz, D_2O): δ 175.85 (CO), 175.07 (NH*C*OCH_3), 174.95 (CO), 174.49 (CO), 172.84 (CO), 144.43 (2C), 144.42, 126.33, 126.24, 126.22, 104.22, 102.28, 80.55, 75.78, 75.61, 74.51, 73.72, 73.62, 73.35, 72.15, 71.92, 69.52, 69.44, 69.38, 68.74, 66.85, 64.42, 63.87, 62.94, 61.98, 61.04, 58.81, 54.72, 53.04, 52.69 (2C), 51.16, 48.84, 37.16, 36.54, 31.09, 31.01, 29.83, 29.69, 23.06, 22.98, 22.85; HRMS (ESI): m/z [M-2H]-2 calcd for C99H155N152O61: 1264.9749, found: 1264.9775.

*4.8 Synthesis of conjugate **11***

Conjugate **11** was obtained through a coupling of propargyl sialoside **8** (7.4 mg, 2.92 μmol) with compound **9** (10 mg, 0.59 μmol) by following the general procedure for CuAAC ligation, in 88% yield (12.8 mg) as an off-white powder after P-2 gel chromatography purification using H_2O as eluent and subsequent lyophilization. Substitution of the PEG scaffold was determined by ^{1}H NMR integration of the underlined peaks to be lactose-3'-sialyllactose:PEG = 4:1. ^{1}H NMR (600 MHz, D_2O): δ 8.03 (s, 5H), 4.93 (broad s, 4H), 4.82 (broad s, 4H), 4.54 (d, *J* = 7.8 Hz, 4H), 4.39 (d, *J* = 7.8 Hz, 4H), 4.19 (dd, *J* = 8.4, 6.0 Hz, 4H), 3.91 (dd, *J* = 10.8, 1.8 Hz, 4H), 3.84-3.80 (m, 4H), 3.77-3.60 (m, 6H), 3.66 (band, PEG C*H*$_2$, 278H), 3.52-3.49 (m, 8H), 3.32 (m, 8H), 3.20-3.24 (m, 2H),3.19-3.10 (m, 2H), 2.84 (broad s, 1H), 2.67 (dd, *J* = 3.6, 12.0 Hz, 3H), 2.60 (m, 1H), 2.51 (broad s, 4H), 2.49 (bs, PEG-COC*H*$_2$C*H*$_2$CO-, 4H), 2.43(m, 1H), 2.07 (broad s, 2H), 1.98 (s, 9H, NHAc), 1.87 (broad s, 4H), 1.75-1.73 (m, 5H), 1.69 (t, *J* = 12.0 Hz, 2H), 1.58-1.46 (m, 2H), 1.33-1.28 (broad, 10H); ^{13}C NMR (126 MHz, D_2O): δ 174.93 (2C's), 174.73, 174.15, 174.04, 173.97, 173.80, 173.70, 173.58, 173.48, 143.66, 125.35, 103.27, 102.98, 102.08, 101.31, 101.30, 100.36, 79.58, 78.47, 75.38, 74.79, 74.72, 74.65, 74.52, 73.71, 72.90, 72.68, 72.57, 72.40, 71.82, 71.76, 70.99, 70.83, 70.71, 70.62, 69.62 (PEG *C*H$_2$-), 69.45, 68.88, 68.58, 68.54, 68.41, 68.38, 67.47, 66.67, 65.91, 63.55, 62.99, 62.68 (2C's), 62.07, 61.05, 60.40, 60.28, 60.16, 57.87, 53.79, 51.83 (2C's), 50.12, 47.81, 45.10, 40.14 (2C's), 38.98 (2C's), 38.65, 36.24,

35.68, 35.60, 31.11 (2C's), 30.55, 30.40, 30.15, 30.04, 28.93, 28.78 (2C's), 28.40, 28.22, 27.91, 25.03, 24.95, 22.10 (2C's), 21.96, 21.94.

*4.9 Synthesis of conjugate **12***

Conjugate **12** was obtained through coupling of propargyl sialoside **8** (6.5 mg, 2.56 μmol) with compound **10** (8 mg, 0.51 μmol) by following the general procedure for CuAAC ligation, in 90% yield (11.9 mg) as an off-white white powder after P-2 gel chromatography purification using eluent system H_2O and lyophilization. Substitution of the PEG scaffold was determined by ^{1}H NMR integration of the underlined peaks to be A-type II-3'-sialyllactose:PEG = 4:1. ^{1}H NMR (600 MHz, D_2O): δ 8.02 (s, 5H), 5.30 (d, J = 4.2 Hz, 1H), 5.14 (d, J = 4.2 Hz, 1H), 4.57-4.52 (m, 2H), 4.39-4.37 (band, 4H), 4.27 (q, J = 6.6 Hz, 1H), 4.18-4.11 (m, 4H), 3.95 (t, J = 3.6 Hz, 2H), 3.93-3.92 (m, 4H), 3.87-3.84 (m, 5H), 3.66 (band, PEG CH_2-, 243H), 3.35-3.32 (m, 4H), 3.18-3.10 (m, 2H), 2.84 (broad s, 1H), 2.67 (dd, J = 3.6, 12.0 Hz, 4H), 2.61-2.57 (m, 1H), 2.54-2.50 (m, 8H), 2.48 (bs, PEG-COCH_2CH_2CO-, 4H), 2.06-2.03 (m, 4H), 1.98 (s, 15H, NHAc), 1.91-1.82 (m, 8H), 1.75-1.73 (m, 6H), 1.69 (t, J = 12.0 Hz, 2H), 1.56-1.44 (m, 2H), 1.33-1.28 (broad, 13H); ^{13}C NMR (126 MHz, D_2O): δ 174.92 174.84, 174.72, 174.14, 173.50(2C's), 143.58, 142.48, 139.46, 129.46, 125.38, 125.29, 125.27, 103.28, 102.98, 101.31, 101.14, 100.34, 100.1, 98.67, 91.36, 79.58 (3C's), 78.39, 79.58, 78.39, 76.29, 76.05, 75.72, 75.38, 75.19, 74.84, 74.72, 74.40, 73.71, 72.68, 72.57, 72.40, 71.82, 71.75, 70.99, 70.83, 70.61, 69.99, 69.88, 69.70, 69.62 (PEG CH_2-), 69.49, 69.45, 68.88, 68.54, 68.41, 67.38, 66.67, 65.91, 63.55, 63.08, 62.68, 62.03, 61.34, 61.20, 61.05, 60.40, 60.29, 59.38, 57.89, 55.47, 53.79 (2C's), 52.95, 51.83 (2C's), 50.10, 50.07, 49.63, 49.54, 47.80, 40.15, 38.98, 36.24, 35.68, 31.10 (2C's), 30.42, 30.14, 28.93, 28.80, 28.60, 28.40, 28.35, 27.97, 25.10, 22.34 (2C's), 22.10, 21.99, 20.50, 16.16.

4.10 Clustering of BCR and CD22 receptors on B cells

A-BCL cells were prepared and grown as previously described.[38] Cells were grown in R10 media supplemented with glutamax and 1% beta-mercaptoethanol added weekly in 12-well plates (Corning, Inc.). Plates were kept in a humidified incubator at 37 °C and 5% CO_2. For fluorescence microscopy experiments, 2 x10^6 cells were washed and treated with 25 ng mL^{-1} of the indicated conjugate on ice for 1 h, then fixed using 1% PFA on ice for 20 min. Samples were treated with 1 μL mL^{-1} mouse anti-human IgM (clone IM260, Abcam) or mouse anti-human CD22 (clone HIB22, BD Pharmingen) at 4 °C overnight, washed, and stained with goat anti-mouse IgG (polyclonal, Sigma-Aldrich) conjugated with Alexa Flour 647 at room temperature for 1 h. The loading of the fluorophores was approximately 2 dye per protein as determined by spectrophotometry. After washing, samples were transferred to 24-well plates (Corning, Inc.) with 12 mm circular cover glass slides pre-treated with 0.001% poly-L-lysine and spun at 300 x g for 15 min. Cover glass slides with samples were washed, mounted onto microscopy slides with Slowfade Antifade (Thermo Fisher), and sealed with Cytoseal 60. Samples were imaged on a laser scanning confocal microscope (Olympus IX81) at 60X. Twenty cells from each condition were chosen for analysis based on transmitted and fluorescence images, in which each image was subjected to similar thresholding levels, and each cluster was analyzed using the particle analysis function on ImageJ. The area of a single pixel in these images was 0.0173 μm^2. The areas of each cluster from the analyses were plotted using bean plot in the R statistical package. Analysis of the means and Student's t-test were performed in GraphPad Prism.

Acknowledgements

The authors would like to thank Prof. Todd L. Lowary and Dr Peter Meloncelli for providing advanced synthetic intermediates for the synthesis of human ABO blood group antigens. This work was supported by grants from the Alberta Glycomics Centre and the

Natural Sciences and Engineering Research Council of Canada (NSERC, RGPIN-2020-04371).

Supplementary data

Supplementary data including NMR spectra for compounds **4**, **6**, **8**, **11**, and **12** can be found online.

Conflicts of interest

The authors declare no conflict of interest.

ORCID

Gour Chand Daskhan, 0000-0002-1805-5750

Hanh-Thuc Ton Tran, 0000-0001-6294-2448

Christopher W Cairo, 0000-0003-3363-8708

References

[1] A. Varki, R.D. Cummings, J.D. Esko, P. Stanley, G.W. Hart, M. Aebi, A.G. Darvill, T. Kinoshita, N.H. Packer, J.H. Prestegard, R.L. Schnaar, P.H. Seeberger, eds., Essentials of Glycobiology, 3rd ed., Cold Spring Harbor Laboratory Press, Cold Spring Harbor (NY), 2015.

[2] C.R. Bertozzi, L.L. Kiessling, Chemical Glycobiology, Science. 291 (2001) 2357–2364. https://doi.org/10.1126/science.1059820.

[3] R.T. Lee, Y.C. Lee, Affinity enhancement by multivalent lectin–carbohydrate interaction, Glycoconj. J. 17 (2000) 543–551. https://doi.org/10.1023/A:1011070425430.

[4] J.J. Lundquist, E.J. Toone, The Cluster Glycoside Effect, Chem. Rev. 102 (2002) 555–578. https://doi.org/10.1021/cr000418f.

[5] M. Mammen, S.-K. Choi, G.M. Whitesides, Polyvalent Interactions in Biological Systems: Implications for Design and Use of Multivalent Ligands and Inhibitors, Angew. Chem. Int. Ed. 37 (1998) 2754–2794. https://doi.org/10.1002/(SICI)1521-3773(19981102)37:20<2754::AID-ANIE2754>3.0.CO;2-3.

[6] C.F. Brewer, M.C. Miceli, L.G. Baum, Clusters, bundles, arrays and lattices: novel mechanisms for lectin–saccharide-mediated cellular interactions, Curr. Opin. Struct. Biol. 12 (2002) 616–623. https://doi.org/10.1016/S0959-440X(02)00364-0.

[7] L.L. Kiessling, N.L. Pohl, Strength in numbers: non-natural polyvalent carbohydrate derivatives, Chem. Biol. 3 (1996) 71–77. https://doi.org/10.1016/S1074-5521(96)90280-X.

[8] L.L. Kiessling, J.E. Gestwicki, L.E. Strong, Synthetic Multivalent Ligands as Probes of Signal Transduction, Angew. Chem. Int. Ed. 45 (2006) 2348–2368. https://doi.org/10.1002/anie.200502794.

[9] S. Cecioni, A. Imberty, S. Vidal, Glycomimetics versus Multivalent Glycoconjugates for the Design of High Affinity Lectin Ligands, Chem. Rev. 115 (2015) 525–561. https://doi.org/10.1021/cr500303t.

[10] L. L. Kiessling, J. C. Grim, Glycopolymer probes of signal transduction, Chem. Soc. Rev. 42 (2013) 4476–4491. https://doi.org/10.1039/C3CS60097A.

[11] M. González-Cuesta, C.O. Mellet, J.M.G. Fernández, Carbohydrate supramolecular chemistry: beyond the multivalent effect, Chem. Commun. 56 (2020) 5207–5222. https://doi.org/10.1039/D0CC01135E.

[12] V. Wittmann, R. J. Pieters, Bridging lectin binding sites by multivalent carbohydrates, Chem. Soc. Rev. 42 (2013) 4492–4503. https://doi.org/10.1039/C3CS60089K.

[13] N. Jayaraman, K. Maiti, K. Naresh, Multivalent glycoliposomes and micelles to study carbohydrate– protein and carbohydrate– carbohydrate interactions, Chem. Soc. Rev. 42 (2013) 4640–4656. https://doi.org/10.1039/C3CS00001J.

[14] A. Bernardi, J. Jiménez-Barbero, A. Casnati, C.D. Castro, T. Darbre, F. Fieschi, J. Finne, H. Funken, K.-E. Jaeger, M. Lahmann, T. K. Lindhorst, M. Marradi, P. Messner, A. Molinaro, P. V. Murphy, C. Nativi, S. Oscarson, S. Penadés, F. Peri, R. J. Pieters, O. Renaudet, J.-L. Reymond, B. Richichi, J. Rojo, F. Sansone, C. Schäffer, W. Bruce Turnbull, T. Velasco-Torrijos, S. Vidal, S. Vincent, T. Wennekes, H. Zuilhof, A. Imberty, Multivalent glycoconjugates as anti-pathogenic agents, Chem. Soc. Rev. 42 (2013) 4709–4727. https://doi.org/10.1039/C2CS35408J.

[15] C.M. Galan, P. Dumy, O. Renaudet, Multivalent glyco(cyclo)peptides, Chem. Soc. Rev. 42 (2013) 4599–4612. https://doi.org/10.1039/C2CS35413F.

[16] D. Goyard, A. Martin-Serrano Ortiz, D. Boturyn, O. Renaudet, Multivalent glycocyclopeptides: conjugation methods and biological applications, Chem. Soc. Rev. 51 (2022) 8756–8783. https://doi.org/10.1039/D2CS00640E.
[17] Y. Kim, J. Young Hyun, I. Shin, Multivalent glycans for biological and biomedical applications, Chem. Soc. Rev. 50 (2021) 10567–10593. https://doi.org/10.1039/D0CS01606C.
[18] B. Lepenies, J. Yin, P.H. Seeberger, Applications of synthetic carbohydrates to chemical biology, Curr. Opin. Chem. Biol. 14 (2010) 404–411. https://doi.org/10.1016/j.cbpa.2010.02.016.
[19] S. Bhatia, M. Dimde, R. Haag, Multivalent glycoconjugates as vaccines and potential drug candidates, MedChemComm. 5 (2014) 862–878. https://doi.org/10.1039/C4MD00143E.
[20] W.C. Chen, G.C. Completo, D.S. Sigal, P.R. Crocker, A. Saven, J.C. Paulson, In vivo targeting of B-cell lymphoma with glycan ligands of CD22, Blood. 115 (2010) 4778–4786. https://doi.org/10.1182/blood-2009-12-257386.
[21] E. Kaltgrad, M.K. O'Reilly, L. Liao, S. Han, J.C. Paulson, M.G. Finn, On-Virus Construction of Polyvalent Glycan Ligands for Cell-Surface Receptors, J. Am. Chem. Soc. 130 (2008) 4578–4579. https://doi.org/10.1021/ja077801n.
[22] E.B. Puffer, J.K. Pontrello, J.J. Hollenbeck, J.A. Kink, L.L. Kiessling, Activating B cell signaling with defined multivalent ligands, ACS Chem. Biol. 2 (2007) 252–262.
[23] A.H. Courtney, E.B. Puffer, J.K. Pontrello, Z.-Q. Yang, L.L. Kiessling, Sialylated multivalent antigens engage CD22 in trans and inhibit B cell activation, Proc. Natl. Acad. Sci. 106 (2009) 2500. https://doi.org/10.1073/pnas.0807207106.
[24] M.S. Macauley, P.R. Crocker, J.C. Paulson, Siglec-mediated regulation of immune cell function in disease, Nat. Rev. Immunol. 14 (2014) 653–666. https://doi.org/10.1038/nri3737.
[25] J. Jellusova, L. Nitschke, Regulation of B Cell Functions by the Sialic Acid-Binding Receptors Siglec-G and CD22, Front. Immunol. 2 (2012). https://www.frontiersin.org/articles/10.3389/fimmu.2011.00096 (accessed May 19, 2023).
[26] G. Murugesan, B. Weigle, P.R. Crocker, Siglec and anti-Siglec therapies, Curr. Opin. Chem. Biol. 62 (2021) 34–42. https://doi.org/10.1016/j.cbpa.2021.01.001.
[27] Z.-Q. Yang, E.B. Puffer, J.K. Pontrello, L.L. Kiessling, Synthesis of a multivalent display of a CD22-binding trisaccharide, Carbohydr. Res. 337 (2002) 1605–1613. https://doi.org/10.1016/S0008-6215(02)00270-7.
[28] H. Kristyanto, M.D. Holborough-Kerkvliet, L. Lelieveldt, Y. Bartels, R. Hammink, K.A.J. van Schie, R.E.M. Toes, K.M. Bonger, H.U. Scherer, Multifunctional, Multivalent PIC Polymer Scaffolds for Targeting Antigen-Specific, Autoreactive B Cells, ACS Biomater. Sci. Eng. 8 (2022) 1486–1493. https://doi.org/10.1021/acsbiomaterials.1c01395.
[29] M.K. O'Reilly, B.E. Collins, S. Han, L. Liao, C. Rillahan, P.I. Kitov, D.R. Bundle, J.C. Paulson, Bifunctional CD22 Ligands Use Multimeric Immunoglobulins as Protein Scaffolds in Assembly of Immune Complexes on B Cells, J. Am. Chem. Soc. 130 (2008) 7736–7745. https://doi.org/10.1021/ja802008q.
[30] L. Cui, P.I. Kitov, G.C. Completo, J.C. Paulson, D.R. Bundle, Supramolecular Complexing of Membane Siglec CD22 Mediated by a Polyvalent Heterobifunctional Ligand that Templates on IgM, Bioconjug. Chem. 22 (2011) 546–550. https://doi.org/10.1021/bc100579d.

[31] K. Loomis, B. Smith, Y. Feng, H. Garg, A. Yavlovich, R. Campbell-Massa, D.S. Dimitrov, R. Blumenthal, X. Xiao, A. Puri, Specific targeting to B cells by lipid-based nanoparticles conjugated with a novel CD22-ScFv, Exp. Mol. Pathol. 88 (2010) 238–249. https://doi.org/10.1016/j.yexmp.2010.01.006.
[32] B. Kim, J. Shin, T. Kiziltepe, B. Bilgicer, Identification of a moderate affinity CD22 binding peptide and in vitro optimization of peptide-targeted nanoparticles for selective uptake by CD22+ B-cell malignancies, Nanoscale. 12 (2020) 11672–11683. https://doi.org/10.1039/D0NR02133D.
[33] O. Cooper, M. Waespy, D. Chen, S. Kelm, Q. Li, T. Haselhorst, J. Tiralongo, Sugar-decorated carbon dots: a novel tool for targeting immunomodulatory receptors, Nanoscale Adv. 4 (2022) 5355–5364. https://doi.org/10.1039/D2NA00364C.
[34] W. Peng, J.C. Paulson, CD22 Ligands on a Natural N-Glycan Scaffold Efficiently Delivers Tox-ins to B-Lymphoma Cells, J. Am. Chem. Soc. 139 (2017) 12450–12458. https://doi.org/10.1021/jacs.7b03208.
[35] H.H.M. Abdu-Allah, K. Watanabe, S. Daikoku, O. Kanie, T. Tsubata, H. Ando, H. Ishida, M. Kiso, Design and Synthesis of a Multivalent Heterobifunctional CD22 Ligand as a Potential Immunomodulator, Synthesis. (2011) 2968–2974. https://doi.org/10.1055/s-0030-1260151.
[36] H. Prescher, A. Schweizer, M. Frank, E. Kuhfeldt, J. Ring, L. Nitschke, Targeting Human CD22/Siglec-2 with Dimeric Sialosides as Novel Oligosaccharide Mimetics, J. Med. Chem. 65 (2022) 10588–10610. https://doi.org/10.1021/acs.jmedchem.2c00765.
[37] G.C. Daskhan, H.-T.T. Tran, P.J. Meloncelli, T.L. Lowary, L.J. West, C.W. Cairo, Construction of Multivalent Homo- and Heterofunctional ABO Blood Group Glycoconjugates Using a Trifunctional Linker Strategy, Bioconjug. Chem. (2018). https://doi.org/10.1021/acs.bioconjchem.7b00679.
[38] A.M. Slaney, I.E. Dijke, M. Jeyakanthan, C. Li, L. Zou, P. Plaza-Alexander, P.J. Meloncelli, J.A. Bau, L.L. Allan, T.L. Lowary, L.J. West, C.W. Cairo, J.M. Buriak, Conjugation of A and B Blood Group Structures to Silica Microparticles for the Detection of Antigen-Specific B Cells, Bioconjug. Chem. 27 (2016) 705–715.
[39] G.C. Daskhan, B. Motyka, R. Bascom, H.T. Tran, K. Tao, L.J. West, C.W. Cairo, Extending the in vivo persistence of synthetic glycoconjugates using a serum-protein binder, RSC Chem. Biol. (2022). https://doi.org/10.1039/D2CB00126H.
[40] B.E. Collins, O. Blixt, A.R. DeSieno, N. Bovin, J.D. Marth, J.C. Paulson, Masking of CD22 by cis ligands does not prevent redistribution of CD22 to sites of cell contact, Proc. Natl. Acad. Sci. U. S. A. 101 (2004) 6104. https://doi.org/10.1073/pnas.0400851101.
[41] V. Dourtoglou, B. Gross, O-Benzotriazolyl-N, N, N', N'-tetramethyluronium hexafluorophosphate as coupling reagent for the synthesis of peptides of biological interest, Synth. Stuttg. (1984) 572–574.
[42] B.E. Collins, O. Blixt, N.V. Bovin, C.-P. Danzer, D. Chui, J.D. Marth, L. Nitschke, J.C. Paulson, Constitutively unmasked CD22 on B cells of ST6Gal I knockout mice: novel sialoside probe for murine CD22, Glycobiology. 12 (2002) 563–571. https://doi.org/10.1093/glycob/cwf067.
[43] H.-T.T. Tran, C. Li, R. Chakraberty, C.W. Cairo, NEU1 and NEU3 enzymes alter CD22 organization on B cells, Biophys. Rep. 2 (2022) 100064. https://doi.org/10.1016/j.bpr.2022.100064.
[44] E.D. Goddard-Borger, R.V. Stick, An Efficient, Inexpensive, and Shelf-Stable Diazotransfer Reagent: Imidazole-1-sulfonyl Azide Hydrochloride, Org. Lett. 9 (2007) 3797–3800. https://doi.org/10.1021/ol701581g.

[45] G.T. Potter, G.C. Jayson, G.J. Miller, J.M. Gardiner, An Updated Synthesis of the Diazo-Transfer Reagent Imidazole-1-sulfonyl Azide Hydrogen Sulfate, J. Org. Chem. 81 (2016) 3443–3446. https://doi.org/10.1021/acs.joc.6b00177.